Acta Cryst. (1999). B**55**, 55–69

Crystal and molecular structures of diazapyrenes and a study of $\pi\cdots\pi$ interactions†

Rudolf Kiralj, Biserka Kojić-Prodić,* Ivo Piantanida and Mladen Žinić

Rudjer Bošković Institute, PO Box 1016, HR-10001 Zagreb, Croatia. E-mail: kojic@rudjer.irb.hr

(*Received 23 January 1998; accepted 6 May 1998*)

Abstract

Two diazapyrenes, 5,10-dimethyl-4,9-diazapyrene (1) and novel 2,7-dimethyl-4,9-diazapyrene (2) have been synthesized. Their crystal structures are reported here and are the first representatives of diazapyrenes. Crystal data: (1) monoclinic, $P2_1/c$, a = 4.0246 (5), b = 15.5147 (5), c = 9.1453 (9) Å, β = 101.23 (1)°, V = 560.1 (1) Å^3, Z = 2, R = 0.043; (2) monoclinic, $C2/m$, a = 12.4968 (3), b = 11.4751 (4), c = 3.9615 (5) Å, β = 96.80 (1)°, V = 564.09 (5) Å^3, Z = 2, R = 0.0405. The experimental bond lengths are compared with those calculated by molecular mechanics (*MM*3), semi-empirical methods (*MOPAC*6.0-*PM*3, *AM*1, *MNDO*) and values predicted by valence-bond and variable-electronegativity self-consistent field (VESCF) methods. $\pi\cdots\pi$ interactions in (1), (2) and seventeen other pyrene and pyrene-like molecules selected from the Cambridge Structural Database [Allen & Kennard (1993). *Chem. Des. Autom. News*, **8**, 131–137] have been studied. The following quantitative parameters of $\pi\cdots\pi$ interactions have been calculated: the shortest crystallographic axis, the offset parameter, the interplanar angle, the interactive volume and the overlapping surfaces. They are used for the classification of crystal-packing motifs; a high predominance of β and a few cases of γ and sandwich-herringbone types are observed. In addition, electronegativity, the sum of partial atomic charges of the ring non-H atoms and the number of aromatic skeleton electrons are used as parameters for classification. *MOPAC-PM*3 was used to calculate the partial atomic charges in (1), (2) and pyrene analogues. Correlations between geometrical and electronic structure parameters reveal an analogy between the β-type structures and the crystal structure of graphite.

1. Introduction

Non-covalent interactions between delocalized π systems of aromatic molecules play a considerable role in molecular recognition and molecular aggregation. $\pi\cdots\pi$ interactions (Hunter, 1994; Hunter & Sanders, 1990) are of interest in structural molecular biology, materials science and host–guest chemistry (D'Souza & Maitra, 1996), and supramolecular chemistry (Webb & Wilcox, 1993). One of the most intriguing phenomena in biology involving $\pi\cdots\pi$ interactions is the intercalation of neutral or charged aromatic compounds between adjacent base pairs of double-stranded DNA (Wilson, 1989; Wakelin, 1986). Various natural (Bailly *et al.*, 1990) or synthetic (Denny *et al.*, 1983; Wilson *et al.*, 1988) intercalators are known. However, numerous problems remain, including the design of a reliable model to predict the strength of the interaction and the preferred intercalation site (Veal *et al.*, 1990; Sponer & Hobza, 1996; Sponer *et al.*, 1996).

The 4,9-diazapyrenes are described here to see how they can be used as DNA intercalators or as DNA base analogues. As there are no structural data available for this class of aromatic system, they are compared with analogous pyrene and pyrene-like molecules.

Among the most efficient and the most thoroughly studied intercalators is the phenanthridine derivative ethidium cation, with a formal positive charge on the phenanthridine N atom [(3) in Fig. 1] (Sobell *et al.*, 1977; Meyer-Almes & Porschke, 1993; Sarfati *et al.*, 1995). Recently, Lehn and coworkers (Blacker *et al.*, 1987) and Brunn & Harriman (1991) described the DNA-intercalation properties of the 2,7-diazapyrenium system. It turned out that this dication is efficient in the cleaving of DNA in visible light (Blacker *et al.*, 1986). These results focused our attention on the isomeric 4,9-diazapyrenium system. Surprisingly, very little is known about the

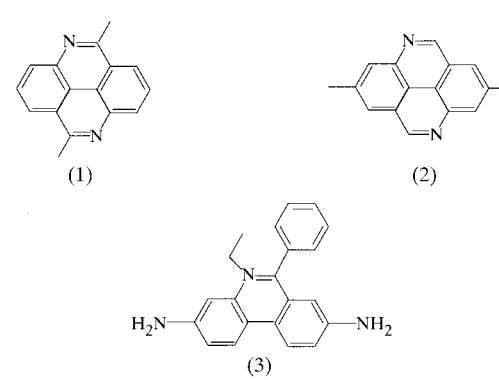

Fig. 1. Chemical diagrams for 5,10-dimethyl-4,9-diazapyrene, (1), 2,7-dimethyl-4,9-diazapyrene, (2), and ethidium, (3).

† This paper was presented orally at The Seventeenth European Crystallographic Meeting, Lisbon, Portugal, 24–28 August 1997.

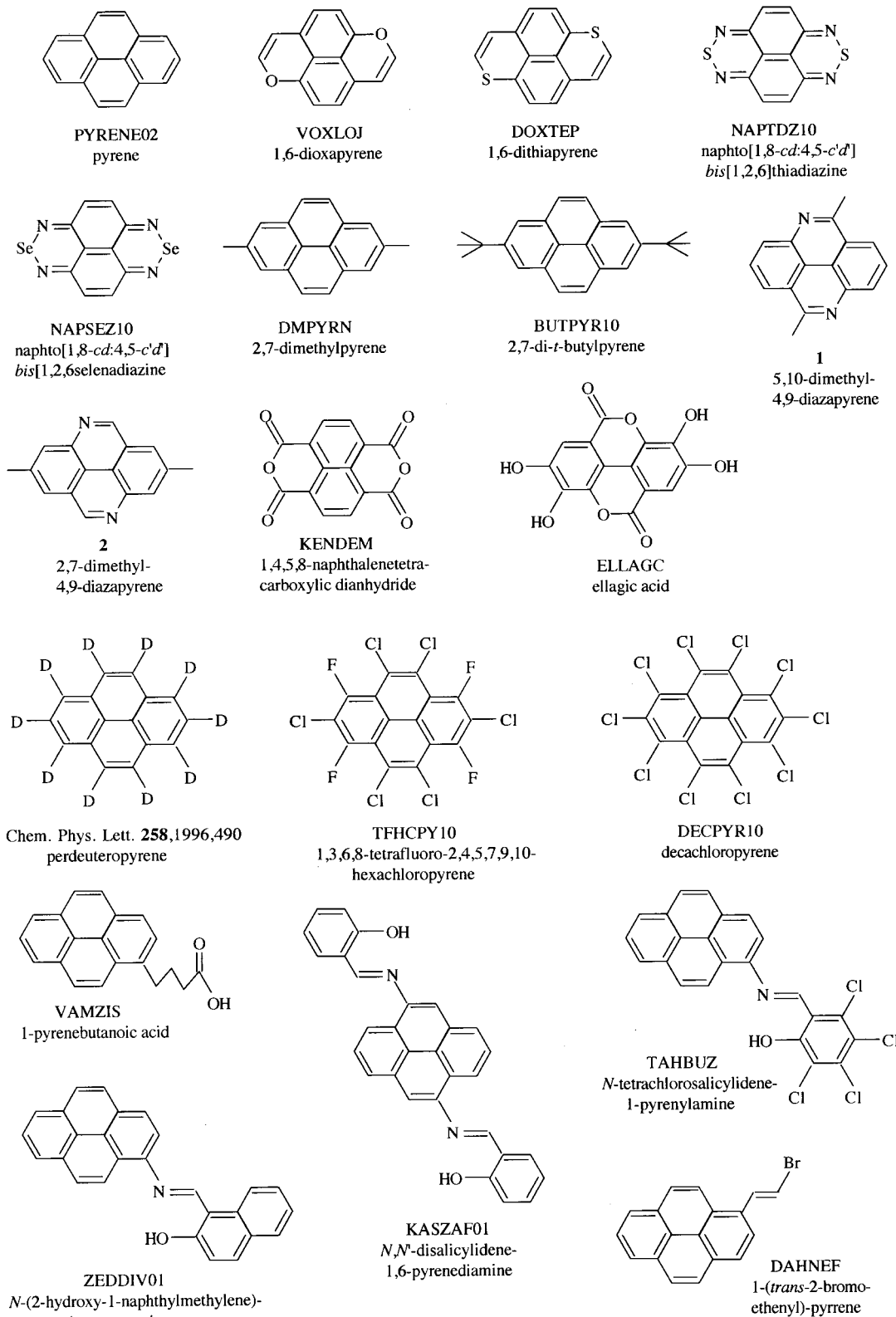

Fig. 2. Chemical diagrams for the compounds used for the analysis with CSD REFCODEs and chemical names.

chemistry, and almost nothing about the biological properties, of 4,9-diazapyrene and its cations; the synthesis of a few representatives was described forty years ago (Fairfull *et al.*, 1952; Badger & Sasse, 1957; Mosby, 1957).

4,9-Diazapyrenes and their derivatives have been studied as part of research related to the synthesis, chemical characterization and biological properties of novel DNA intercalators and potential DNA base analogues (Piantanida, 1997). Some of the 4,9-diazapyrenium compounds were recognized to be very potent in inducing apoptosis in human tumour cells, whereas this effect was small on normal cells (Steiner-Biočić *et al.*, 1996). These interesting biological properties and the fact that they were studied very little in the past justify our work.

The crystal packing, based on stacked layers, is analysed as a model for $\pi\cdots\pi$ interactions effective in intercalation using the crystal structures of 5,10-dimethyl-4,9-diazapyrene, (1), its 2,7-dimethyl analogue, (2), (Fig. 1) and seventeen pyrene derivatives and pyrene-like systems (Fig. 2) extracted from the Cambridge Structural Database (CSD; Allen & Kennard, 1993). The crystal structures were classified according to the approach given by Desiraju and Gavezzotti (Gavezzotti & Desiraju, 1988; Desiraju & Gavezzotti, 1989) indicating $\pi\cdots\pi$ interactions between neighbouring molecules. The quantitative analysis of this interaction was based on the offset parameter, the interplanar angle, overlapping surfaces (stacking areas), the interactive volume and the shortest crystallographic axis (Fig. 3), as well as the average atomic electronegativity after Pauling (Shriver *et al.*, 1990), the number of delocalized, localized and free electrons, and the sum of the partial atomic charges of the non-H ring atoms of the sixteen pyrene skeleton atoms [obtained using *MOPAC-PM*3 (Stewart, 1990*a*,*b*; MOPAC, 1990)].

The interaction energy between adjacent molecules in the crystal was evaluated using the empirical potential given by Gavezzotti (1994) and the program *PLUTO* (Motherwell, 1997) implemented in the CSD. The relationships between bond lengths and bond orders for C—C and C—N bonds of diaza- and polyazabenzenoids, computed by valence-bond and molecular-orbital methods, were found using linear-regression analysis. The molecular structures of (1) and (2) were reproduced by molecular mechanics and semi-empirical methods and were compared with experimental data.

2. Experimental

2.1. *Preparation of (1) and (2)*

5,10-Dimethyl-4,9-diazapyrene, (1), previously described by Mosby (1957) and novel 2,7-dimethyl-4,9-diazapyrene, (2), were prepared by the modified Mosby procedure (1957). 2,2′-Diacetamidobiphenyl or 2,2′-diformamido-4,4′-dimethylbiphenyl (Piantanida, 1997) (3 mmol) was mixed with anhydrous $AlCl_3$ (113 mmol) and NaCl (60 mmol), and heated to melt at 523–543 K. The melt was heated for 2 h at this temperature under vigorous stirring. After cooling to 423 K, the melt was poured onto ice (100 g) and made alkaline (pH 10) with 5 mol dm^{-3} NaOH. The precipitate was collected, dried and subjected to continuous extraction with $CHCl_3$ for 20 h. The solvent was evaporated and the solid residue purified by column chromatography on silica gel using 5% MeOH in CH_2Cl_2 as eluant. Recrystallizations from $CHCl_3$ gave (1) and (2) in 15 and 20% yield, respectively. Data for (1): ^{1}H NMR (300 MHz, $CDCl_3$): 3.19 (6H, *s*), 8.17 (2H, *t*), 8.40 (2H, *d*), 8.51 (2H, *d*). Data for (2): m.p. 523–525 K; IR (KBr): 3000, 1570, 1460, 1410, 1305, 1268, 930 cm^{-1}; ^{1}H NMR (300 MHz, $CDCl_3$): 2.89 (6H, *s*), 8.22 (2H, *s*), 8.49 (2H, *s*), 9.64 (2H, *s*); HRMS (FAB): calculated for $C_{16}H_{12}N_2$ (M^+) 232.100, found 232.099; analysis of $C_{16}H_{12}N_2$: calculated C 82.73, H 5.21, N 12.06; found C 82.89, H 5.33, N 12.23%.

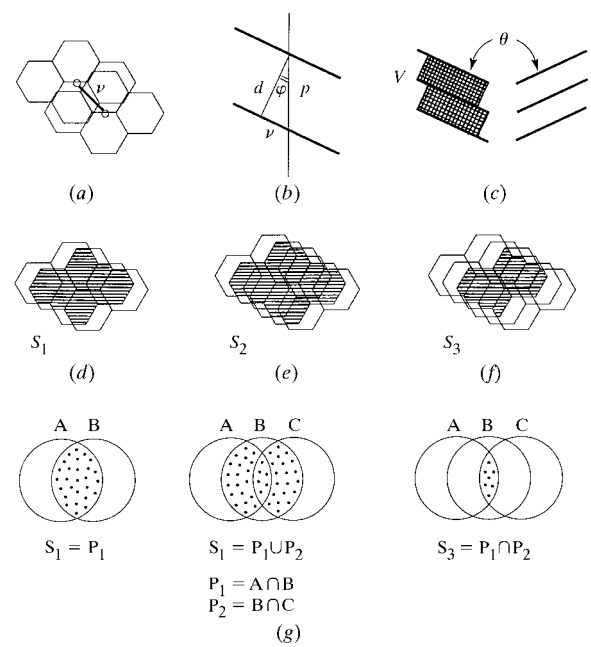

Fig. 3. Geometrical parameters used for the definition and classification of packing types of pyrenes and analogues: (*a*) 'centre-to-centre' offset v (Å), (*b*) interplanar distance d (Å), the shortest axis p (Å) and the angle φ (°); (*c*) interplanar angle θ (°) between adjacent stacks, interactive volume $V = 2S_2d$ (Å^3) which defines a space between the reference molecule and its two closest neighbours in the stack; overlapping surfaces of the reference molecule viewed perpendicular to the least-squares planes of the aromatic rings with (*d*) a single neighbour, S_1 (Å^2), (*e*) two neighbours, S_2 (Å^2) and (*f*) three neighbours, S_3 (Å^2); (*g*) the overlapping surfaces were calculated as the areas of intersecting polygons with their definition using set theory; the reference molecule is represented as the set B and intersections S_1, S_2, and S_3 of the three sets are equivalent to S_1, S_2, and S_3.

2.2. *Electronic absorption and fluorescence emission spectra of (1) and (2)*

The electronic absorption spectra of the isomeric dimethyl-4,9-diazapyrene derivatives (1) and (2) recorded in EtOH at concentrations of 1.86×10^{-5} and 1.84×10^{-5} mol dm^{-3}, respectively, are shown in Fig. 4. The following absorptions (λ_{max}, nm; ε_{max}) are observed: (1): 243.1 (49408), 257.9 (16451), 268.7 (16505), 321.9 (12258), 336.7 (14667), 364.7 (3871), 376.0 (2849), 384.1 (7634); (2): 238.5 (48967), 258.9 (20760), 269.1 (30652), 317.1 (13260), 330.9 (15054), 351.9 (5706), 370.5 (10380). The spectra of (1) and (2) are similar. However, a bathochromic shift on going from (1) to (2) was observed, particularly in the 300–400 nm region. The spectra of both (1) and (2) exhibit enhanced hypochromic effects with increasing concentration. The concentration–absorption behaviour at selected wavelengths shows clear deviation from linearity above concentrations of 1×10^{-4} mol dm^{-3} for (1) and above 2×10^{-4} mol dm^{-3} for (2). These effects point to the strong tendency of both (1) and (2) to form stacked aggregates in solution.

The fluorescence emission spectra of (1) ($c = 7.19 \times 10^{-6}$ mol dm^{-3}) and (2) ($c = 9.18 \times 10^{-6}$ mol dm^{-3}) dissolved in ethanol are shown in Fig. 5 and confirm the effect of the substitution pattern on the electronic absorption and fluorescence properties of the 4,9-diazapyrene system.

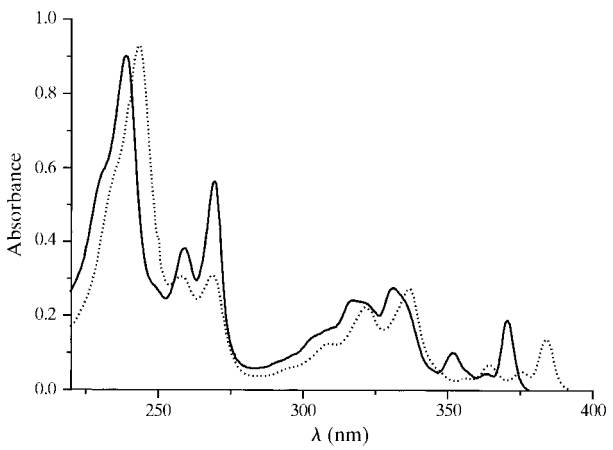

Fig. 4. UV/VIS spectra (EtOH) of compounds (1) (dashed line) and (2) (solid line); $c = 1.86 \times 10^{-5}$ and 1.84×10^{-5} mol dm^{-3}, respectively.

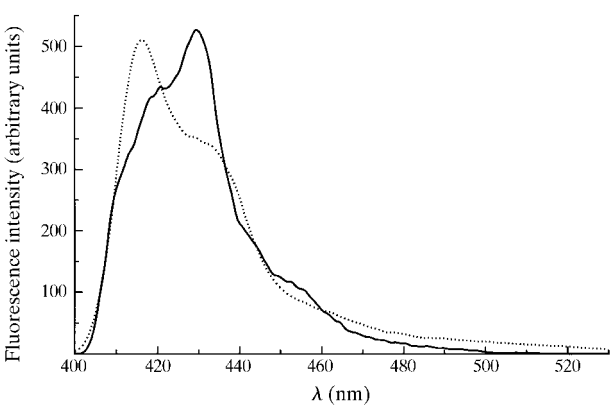

Fig. 5. Fluorescence spectra (EtOH) of compounds (1) (dashed line, $c = 7.19 \times 10^{-6}$ mol dm^{-3}) and (2) (solid line, $c = 9.18 \times 10^{-6}$ mol dm^{-3}).

2.3. *Crystal structure determinations of (1) and (2)*

Crystal data, including data collection parameters and details of the structure refinements, are listed in Table 1. Light-sensitive crystals of (1) were grown in the dark at room temperature from a mixture of dichloromethane and dimethyl sulfoxide. Dichloromethane was used for the crystallization of (2). Data were collected at room temperature and, for (1), in the dark. Data collection and cell refinement were carried out using *CAD*-4 *EXPRESS* (Enraf–Nonius, 1992). Data reduction was performed with the program *HELENA* (Spek, 1990*b*). The structures were solved by direct methods (*SHELXS*86) (Sheldrick, 1990) and refined with *SHELXL*93 (Sheldrick, 1993) on F^2. Scattering factors were from *SHELXL*93. The H-atom coordinates of both compounds were determined from difference Fourier maps with the exception of those of the methyl groups in (2), which were calculated on stereochemical grounds. All H-atom positions were refined. The molecules (1) and (2) have a crystallographic inversion centre in the middle of the C11—C11*a* bond (Figs. 6 and 7). The crystallographic symmetry of molecule (2) is C_{2h}. In

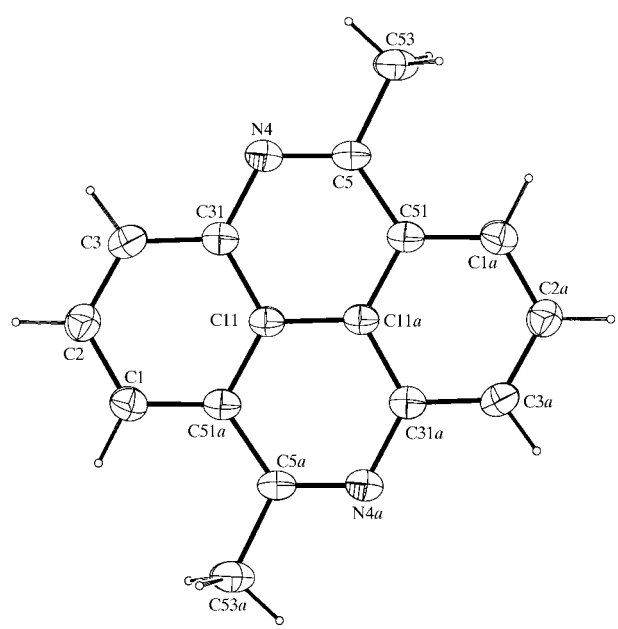

Fig. 6. Molecular structure of (1) [*ORTEP*II (Johnson, 1976), 30% probability level ellipsoids] with the atom numbering (according to *Chemical Abstracts*); symmetry code: (*a*) $-x, 1-y, -z$.

Table 1. *Experimental details*

	(1)	(2)
Crystal data		
Chemical formula	$C_{16}H_{12}N_2$	$C_{16}H_{12}N_2$
Chemical formula weight	232.286	232.286
Cell setting	Monoclinic	Monoclinic
Space group	$P2_1/c$	$C2/m$
a (Å)	4.0246 (5)	12.4968 (3)
b (Å)	15.5147 (5)	11.4751 (4)
c (Å)	9.1453 (9)	3.9615 (3)
β (°)	101.23 (1)	96.80 (1)
V (Å^3)	560.1 (1)	564.09 (5)
Z	2	2
D_x (Mg m^{-3})	1.377	1.369
Radiation type	Cu $K\alpha$	Cu $K\alpha$
Wavelength (Å)	1.54184	1.54184
No. of reflections for cell parameters	18	21
θ range (°)	11–42	10.54–42.56
μ (mm^{-1})	0.6	0.6
F_{000}	244	244
Temperature (K)	295 (3)	295 (2)
Crystal form	Needle	Prism
Crystal size (mm)	0.3 × 0.04 × 0.04	0.32 × 0.14 × 0.11
Crystal colour	Colourless	Colourless
Data collection		
Diffractometer	Enraf–Nonius CAD-4	Enraf–Nonius CAD-4
Data collection method	$\omega/2\theta$ scans	$\omega/2\theta$ scans
Absorption correction	None	None
No. of measured reflections	1297	1108
No. of independent reflections	1135	508
No. of observed reflections	425	322
Criterion for observed reflections	$I > 2\sigma(I)$	$I > 2\sigma(I)$
R_{int}	0.0360	0.0425
θ_{max} (°)	74.19	65.21
Range of h, k, l	$-5 \rightarrow h \rightarrow 0$ $-19 \rightarrow k \rightarrow 0$ $-11 \rightarrow l \rightarrow 11$	$0 \rightarrow h \rightarrow 4$ $-9 \rightarrow k \rightarrow 9$ $-9 \rightarrow l \rightarrow 9$
No. of standard reflections	3	3
Frequency of standard reflections	Every 41 reflections	Every 44 reflections
Refinement		
Refinement on	F^2	F^2
$R[F^2>2\sigma(F^2)]$	0.0425	0.0405
$wR(F^2)$	0.1281	0.1237
S	0.660	1.055
No. of reflections used in refinement	660	508
No. of parameters used	106	70
H-atom treatment	All H-atom parameters refined	All H-atom parameters refined
Weighting scheme	$w = 1/[\sigma^2(F_o^2) + (0.1673P)^2 + 0.5865P]$ where $P = (F_o^2 + 2F_c^2)/3$	$w = 1/[\sigma^2(F_o^2) + (0.0966P)^2 + 0.0939P]$ where $P = (F_o^2 + 2F_c^2)/3$
$(\Delta/\sigma)_{max}$	−0.031	0.005
$\Delta\rho_{max}$ (e Å^{-3})	0.138	0.19
$\Delta\rho_{min}$ (e Å^{-3})	−0.147	−0.12
Extinction method	None	None

order to satisfy the symmetry, positional disorder of the atoms N4 and C4 (Fig. 7) with 50% population at each site occurred.

The molecular geometry was calculated using the program package *PLATON*93 (Spek, 1990*a*). Drawings were prepared using *PLUTON* (Spek, 1991) and *ORTEP*II (Johnson, 1976). Final atomic coordinates and equivalent isotropic displacement parameters are listed in Table 2 for (1) and Table 3 for (2).† Calculations were performed on the Silicon Graphics INDIGO2 work-

† Supplementary data for this paper are available from the IUCr electronic archives (Reference: NA0085). Services for accessing these data are described at the back of the journal.

Table 2. *Fractional atomic coordinates and equivalent isotropic displacement parameters (Å^2) for (1)*

$U_{eq} = (1/3)\Sigma_i\Sigma_j U^{ij} a^i a^j \mathbf{a}_i.\mathbf{a}_j$.

	x	y	z	U_{eq}
N4	0.1676 (8)	0.35583 (19)	0.1291 (3)	0.0470 (11)
C1	0.4509 (10)	0.6138 (3)	0.2271 (4)	0.0500 (17)
C2	0.5860 (11)	0.5469 (3)	0.3198 (4)	0.0536 (16)
C3	0.4908 (11)	0.4623 (3)	0.2872 (4)	0.0530 (17)
C5	−0.0548 (10)	0.3387 (2)	0.0075 (4)	0.0454 (14)
C11	0.1207 (9)	0.5102 (3)	0.0649 (3)	0.0395 (12)
C31	0.2587 (10)	0.4415 (3)	0.1597 (4)	0.0444 (12)
C51	−0.2135 (10)	0.4036 (2)	−0.0975 (4)	0.0435 (12)
C53	−0.1415 (15)	0.2452 (3)	−0.0233 (6)	0.062 (2)

Table 3. *Fractional atomic coordinates and equivalent isotropic displacement parameters (Å^2) for (2)*

$U_{eq} = (1/3)\Sigma_i\Sigma_j U^{ij} a^i a^j \mathbf{a}_i.\mathbf{a}_j$.

	x	y	z	U_{eq}
N4	0.0454 (9)	0.2129 (8)	0.940 (3)	0.067 (5)
C1	0.20167 (13)	0.10471 (15)	0.7671 (4)	0.0577 (6)
C2	0.25315 (17)	0	0.7111 (6)	0.0574 (8)
C4	0.0510 (9)	0.2091 (11)	0.953 (4)	0.064 (5)
C11	0.05070 (15)	0	0.9407 (5)	0.0456 (7)
C21	0.3642 (2)	0	0.5974 (9)	0.0764 (11)
C51	0.10093 (12)	0.10675 (14)	0.8818 (4)	0.0512 (6)

station of the Laboratory for Chemical Crystallography and Biocrystallography, Rudjer Bošković Institute, Zagreb, Croatia.

2.4. *Computational methods*

For the investigation of the bond length–bond order relationships of C—C and C—N bonds in aza-, diaza- and polyazabenzenoids, only the crystal structures of (1) and (2) (this work) are available. Thus, the crystal structures of analogous molecules such as polyazabenzenoids, pyrenes and pyrene-like systems (Fig. 2), and also molecular complexes of pyrene with other aromatic systems, with $R \leq 0.07$ were extracted from the CSD (Allen & Kennard, 1993). Only the best quality data free from error and disorder, without charged species, solvents, clathrates, metal complexes or organometallic compounds were chosen. For the substituted pyrene-like molecules, only terminal groups attached by single bonds were used. As a single example of a non-planar molecule, the structure of decachloropyrene (Hazell & Jagner, 1976) was considered. Data extracted from the CSD were also used for the crystal-packing classification.

C—C and C—N π-bond orders (Kiralj *et al.*, 1996, 1998) for azabenzenoids (Table 4) were calculated by the variable-electronegativity self-consistent field (VESCF) procedure (Allinger *et al.*, 1967) for aromatic systems included in *MM*3(92) (Allinger, 1992). The molecular geometries of (1) and (2) were reproduced by molecular mechanics using *MM*3(92) and by semi-empirical methods using *MOPAC*6.0 (Stewart, 1990*a*,*b*; MOPAC, 1990) with *PM*3 (Stewart, 1989*a*,*b*; Dewar *et al.*, 1990; Stewart, 1990*a*,*b*), *AM*1 (Dewar *et al.*, 1985) and *MNDO* (Dewar & Thiel, 1977) Hamiltonians and PRECISE and EF keywords (Table 5). *PM*3 was used to determine partial atomic charges for (1), (2) (Fig. 1), and all the pyrene-like molecules (Fig. 2). The advantage of *PM*3 over *MNDO* and *AM*1 is that, apparently, (i) it reproduces bond lengths and heats of formation reliably, as we found for phenanthrene (Kiralj *et al.*, 1996), diazapyrenes (1) and (2) and pyrene-like molecules, and (ii) partial atomic charges of the pyrene skeleton calculated by *PM*3 are in between *MNDO* and *AM*1 values and can serve for comparison. Regression equations were established and used to evaluate relationships between the bond lengths and the bond orders of diaza- and polyazabenzenoids, and to correlate the molecular and crystal-packing properties of (1), (2) and pyrene-like systems (Table 6) using *CricketGraph* (Stat Works, 1988).

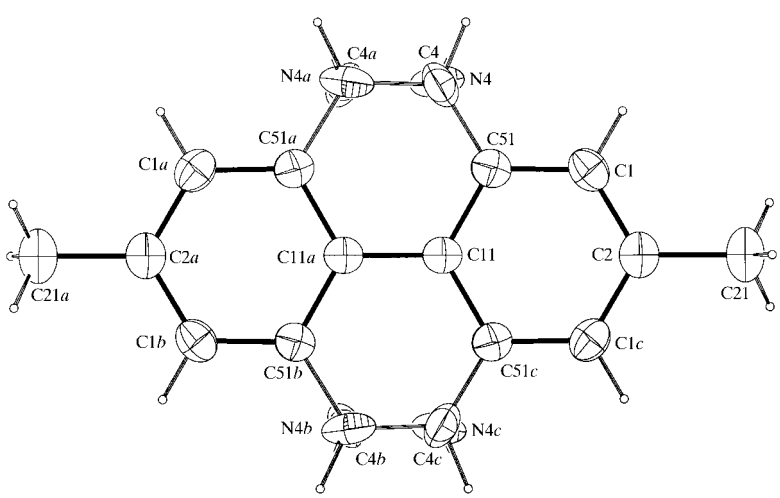

Fig. 7. Molecular structure of (2) [*ORTEP*II (Johnson, 1976), 30% probability level ellipsoids] with the atom numbering (according to *Chemical Abstracts*) and C4, N4 disordered atoms (population parameter = 0.5 for each atom); symmetry codes: (*a*) $-x, y, 2-z$; (*b*) $-x, -y, 2-z$; (*c*) $x, -y, z$.

Table 4. *The results of linear-regression analysis of bond length–bond order relationships for C—C and C—N bonds in aza-, diaza- and polyazabenzenoids*

Pauling's (p_P) and VESCF (p_{VESCF}) π-bond orders. The regression coefficients (a) and (b) are from the regression equation $d = a - bp$, where p is the π-bond order and r is the corresponding correlation coefficient. The average deviation (δ) is calculated from the experimental bond lengths.

Data set	Bond order	No. of data	a (Å)	b (Å)	r	δ (Å)
Benzenoid hydrocarbons†	p_P^{CC}	147	1.464	−0.132	0.806	0.013
	p_{VESCF}^{CC}	147	1.508	−0.175	0.883	0.011
Azabenzenoids†	p_P^{CC}	77	1.462	−0.143	0.783	0.013
	p_{VESCF}^{CC}	77	1.497	−0.161	0.758	0.015
	p_P^{CN}	11	1.444	−0.184	0.959	0.006
	p_{VESCF}^{CN}	11	1.493	−0.219	0.966	0.007
Diazabenzenoids	p_P^{CC}	87	1.458	−0.143	0.897	0.010
	p_{VESCF}^{CC}	87	1.509	−0.185	0.897	0.010
	p_P^{CN}	30	1.415	−0.152	0.962	0.005
	p_{VESCF}^{CN}	30	1.454	−0.178	0.972	0.005
Polyazabenzenoids‡	p_P^{CN}	15	1.431	−0.188	0.779	0.017
	p_{VESCF}^{CN}	15	1.476	−0.217	0.854	0.030

† Kiralj *et al.* (1996, 1998). ‡ Insufficient data for the regression analysis for C—C bonds.

Crystal-packing parameters for pyrene-like systems were calculated using the programs *PLATON* (Spek, 1990*a*) and *PLUTON* (Spek, 1991).

The crystal-packing interactions between the pairs of aromatic molecules in the crystals of pyrene, molecular complexes of pyrene with small aromatic systems and pyrene-like systems from the CSD including (1) and (2) were analysed using *PLUTO* (Motherwell, 1997).

3. Results and discussion

3.1. *Molecular structures of two diazapyrenes and bond length–bond order relationships for aza-, diaza and polyazabenzenoids*

The molecular structures of (1) (Fig. 6) and (2) (Fig. 7) determined by X-ray structure analysis were also evaluated by theoretical methods. To predict the bond lengths in aromatic systems correctly, the bond orders were determined. The results of linear-regression analysis on bond lengths (d) and bond orders (p) for aza-, diaza- and polyazabenzenoids are summarized in Table 4. The largest error (0.030 Å, Table 4) was detected in polyazabenzenoids for the C—N bond calculated by the VESCF approach. In general, both methods, valence-bond and molecular-orbital (using VESCF for aromatic systems), are suitable for predicting bond lengths in aromatic systems with nitrogen as a heteroatom (Kiralj *et al.*, 1996, 1998).

C—C bond lengths in the diazapyrenes (1) and (2) and in pyrene (Hazell *et al.*, 1972) are comparable. Experimental C—C and C—N bond lengths of (1) and (2) are compared with the values calculated by molecular mechanics (*MM*3) and semi-empirical methods (*PM*3, *AM*1 and *MNDO*) in Table 5. The comparison also includes predicted values obtained from regression analysis (*d versus p*) based on valence-bond (VB) (Herndon, 1974; Herndon & Párkányi, 1976) and VESCF [Kiralj *et al.* (1998); procedure for the conjugated system incorporated in *MM*3(92)] approaches. For molecules (1) and (2) (Table 5) the bond lengths calculated by both methods are comparable with the experimental values and optimized geometries from molecular mechanics and semi-empirical methods. Generally, good agreement between the experimentally determined values and the calculated values is observed; differences are mainly within three standard deviations of the experimentally determined parameters, with the exception of the C2—C21 bond of (2) in *PM*3 and *AM*1. For the C_{Ar}—Me single bonds C5—C53 in (1) and C2—C21 in (2), the Pauling potential equation (Pauling, 1980) is used. It reproduces bond lengths for zero bond order much better than the regression equations (Kiralj *et al.*, 1998). The predicted values of bond lengths match the experimental values (Table 5).

Table 5. *Bond lengths (Å) of (1) and (2) obtained by X-ray structure analysis, molecular mechanics, semi-empirical methods and from regression analysis*

	(1) X-ray	(2) X-ray	(1) *MM3*	(2) *MM3*	(1) *PM3*	(2) *PM3*	(1) *AM1*	(2) *AM1*	(1) *MNDO*	(2) *MNDO*	(1), (2) VB†	(1) VESCF‡	(2) VESCF‡
C1—C2	1.383 (6)	1.393 (2)	1.398	1.404	1.399	1.398	1.395	1.401	1.408	1.418	1.387	1.385	1.385
C2—C3	1.383 (7)	—	1.398	1.404	1.392	1.398	1.392	1.399	1.404	1.414	1.387	1.386	1.386
C3—C31	1.383 (5)	—	1.399	1.400	1.400	1.398	1.412	1.409	1.417	1.416	1.387	1.391	1.391
C31—N4	1.393 (5)	—	1.402	1.405	1.412	1.412	1.398	1.404	1.399	1.405	1.413	1.389	1.389
C51—N4	—	1.434 (10)	1.402	1.405	1.412	1.412	1.398	1.404	1.399	1.405	1.413	1.389	1.389
N4—C5	1.312 (5)	—	1.306	1.304	1.317	1.308	1.314	1.305	1.317	1.312	1.291	1.299	1.298
N4—C4*a*	—	1.324 (16)	1.306	1.304	1.317	1.308	1.314	1.305	1.317	1.312	1.291	1.299	1.298
C5—C51	1.451 (5)	—	1.457	1.451	1.459	1.452	1.466	1.457	1.477	1.467	1.434	1.443	1.439
C4—C51	—	1.375 (13)	1.457	1.451	1.459	1.452	1.466	1.457	1.477	1.467	1.434	1.443	1.439
C31—C11	1.417 (6)	—	1.410	1.410	1.411	1.411	1.426	1.425	1.429	1.427	1.410	1.404	1.405
C1—C51*a*	1.396 (5)	—	1.406	1.402	1.396	1.394	1.397	1.394	1.413	1.409	1.387	1.392	1.395
C1—C51	—	1.388 (2)	1.399	1.400	1.400	1.398	1.412	1.409	1.417	1.416	1.387	1.391	1.391
C11—C51*a*	1.405 (6)	—	1.409	1.406	1.410	1.408	1.414	1.413	1.432	1.428	1.410	1.402	1.404
C11—C51	—	1.408 (2)	1.409	1.406	1.410	1.408	1.414	1.413	1.432	1.428	1.410	1.402	1.404
C11—C11*a*	1.416 (4)	1.403 (3)	1.423	1.424	1.429	1.429	1.430	1.430	1.429	1.443	1.410	1.429	1.428
C2—C21	—	1.509 (3)	—	1.508	—	1.487	—	1.483	—	1.507	1.504	—	1.497
C5—C53	1.506 (6)	—	1.511	—	1.494	—	1.499	—	1.515	—	1.504	1.509	—

Symmetry code for (1): (*a*) $-x, 1-y, -z$; for (2): (*a*) $-x, y, 2-z$. † Regression equation used for C—N bonds is $d = 1.444 - 0.184p_P$ and for C—C bonds $d = 1.458 - 0.143p_P$. For single bonds C2—C21 and C5—C53 the Pauling equation is used (Pauling, 1980): $d = 1.504 - 0.3128p_P/(0.84p_P + 1)$. ‡ Regression equation used for C—N bonds is $d = 1.454 - 0.178p_{VESCF}$ and for C—C bonds $d = 1.509 - 0.185p_{VESCF}$.

However, there are discrepancies for structure (2) (Table 5) involving the bonds next to the disordered atoms N4 and C4. The experimental value of the C4—C51 bond length [1.375 (13) Å] is shorter whereas the C51—N4 bond [1.434 (10) Å] is longer than the theoretically derived values.

3.2. *Crystal packing and $\pi\cdots\pi$ interactions of the diazapyrenes and pyrene-like molecules*

3.2.1. *Classification of the crystal packings of condensed polycyclic aromatic hydrocarbons*. In the search for correlations between the molecular structure and molecular packing in crystals some parameters of geometrical and electronic structures may be defined; molecular properties are related to these parameters, while many crystal properties are the consequence of crystal-packing characteristics and intermolecular interactions. Organic compounds rich in π aromatic systems develop certain types of crystal packings, first classified by Robertson (1951). Since then, a large collection of valuable and accurate crystal structure data has been stored in the CSD, and more precise classifications based on accurate data have become possible.

Gavezzotti and Desiraju (Gavezzotti & Desiraju, 1988; Desiraju & Gavezzotti, 1989) have recognized four characteristic crystal-packing patterns of planar condensed polycyclic aromatic hydrocarbons: herringbone (HB), sandwich-herringbone (SH), β type and γ type (Figs. 8*a–c*). The main distinguishing factor among the motifs is the relative orientation of the molecular planes in the crystal, which influences the length of the shortest cell axis p (Fig. 3). The HB type is characterized by the closest molecules oriented in a nonparallel fashion and the shortest axis in the range 5.4–8.0 Å. In the sandwich-herringbone motif (Fig. 8*a*) there are sandwich-like pairs organized in herringbone fashion with the shortest axis longer than 8 Å. The β type (Fig. 8*b*) is characterized by a short axis of about 4 Å with the stacked molecules resembling graphite layers (which are separated by about 3.35 Å; Wells, 1975). One of the two closest layers is translated and its shift is defined by the centre-to-centre offset vector (Fig. 3). In graphite, its value is 1.42 Å, being close to the C—C bond in benzene, 1.394 (7) Å. Goddard *et al.* (1995) introduced the centre-to-centre offset vector for detecting $\pi\cdots\pi$ interactions. In general, the shortest values of the offset parameter are typical of the β motif (*e.g.* 1.48 Å in tetrabenzoheptacene; Goddard *et al.*, 1995). The offset parameter values plausibly reveal the highest degree of $\pi\cdots\pi$ interactions in the β pattern. The γ type (Fig. 8*c*) comprises parallel-displaced molecules with the shortest axis in the range 4.6–5.4 Å. According to the analysis of 32 structures of polycyclic aromatic hydrocarbons given by Desiraju & Gavezzotti (1989) the essential parameter for the crystal-packing classification is the shortest cell axis always being a screw-axis direction in monoclinic or orthorhombic space groups. Kitaigorodsky (1973) found that preferred space groups are those which allow close packing with molecules of C_i symmetry such as $P\bar{1}$, $P2_1/c$ (or equivalents), $C2/c$ or orthorhombic $Pbca$. Goddard *et al.* (1995) detected only two space groups, $P2_1/c$ (or equivalents) and $C2/c$ for the planar polycyclic aromatic hydrocarbons.

3.2.2. *Crystal packing of (1), (2) and pyrene analogues*. The molecular overlap in crystals of (1) and (2) is shown in Figs. 9(*a*) and 9(*b*), respectively. The crystal packings of the β type are shown for (1) and (2) in Figs. 10(*a*) and

10(*b*), respectively. The essential parameters for the classification of the packing type of the molecules in Fig. 2 are listed in Table 6. Two categories of parameters are used. Geometrical parameters are defined in Fig. 3: φ, θ and d are the parameters taken from Goddard *et al.* (1995) whereas stacking areas and interactive volume are defined in this work. The elements of electronic structure used in the analysis are mentioned in §1.

In the 'sample' subjected to analysis, the space group $P2_1/c$ (or $P2_1/a$ and $P2_1/n$) prevails (~85%) with high domination of the β motif, including the diazapyrenes (1) and (2). The classification according to the shortest axis (parallel to the monoclinic twofold axis) is strictly valid for the class of pyrene and its analogues. For packings of the β type the shortest axis value is on average 0.4 Å longer than the sum of the van der Waals radii. Stacking typical of pyrene and analogous systems also occurs between conjugated systems (Fig. 2, Table 6) such as 1,6-dioxopyrene (VOXLOJ), ellagic acid (ELLAGC), naphtho[1,8-*c,d*:4,5-*c′,d′*]bis[1,2,6]selenadiazine (NAPSEZ10) and its sulfur analogue (NAPTDZ10). Among the structures studied, two cases of quasi-β type were detected: the structure of decachloropyrene (β*) (DECPYR10) and *N*-tetrachlorosalicylidene-1-pyrenylamine stacked by salicylidene moiety (β**) (TAHBUZ). An influence of the additional conjugated system to the aromatic one on the crystal-packing motif can be recognized in the crystal structures of nitrobenzene derivatives; their crystal-packing motif is classified as the pseudo-herringbone pattern (André *et al.*, 1997*a*,*b*). The molecule of decachloropyrene was selected as a single example of a nonplanar system also stacked with an average separation distance of 3.715 (3) Å, whereas in TAHBUZ the separation is 3.673 (8) Å. The common characteristic of the pyrene analogues with β-type stacking is the tilt angle φ (Fig. 3) of 60 ± 4°. Owing to the diads in the sandwich-herringbone pattern, this angle is small ($\simeq$ 16°, Fig. 8*a*). However, in this packing the centres of the molecules are on a line which does not coincide with the crystallographic axis; an angle of about 60° between this line and the normal to the plane of the aromatic ring characterizes the sandwich-herringbone pattern. In the γ type (Fig. 8*c*) $\varphi \simeq 45°$. The β type is also characterized by a short offset vector v (Fig. 3, Table 6). In many cases, the offset vector is collinear with the molecular elongation axis. Diagonal sliding can be influenced by the presence of polar ring heteroatom(s) (Table 6, O in VOXLOJ, S in DOXTEP), small substituents as in 2,6-dimethylpyrene (Fig. 2, DMPYRN) and steric hindrance as in the crystal packing of 1,3,6-tetrafluoro-2,4,5,7,9,10-hexachloropyrene and decadeuteropyrene (Fig. 2, Table

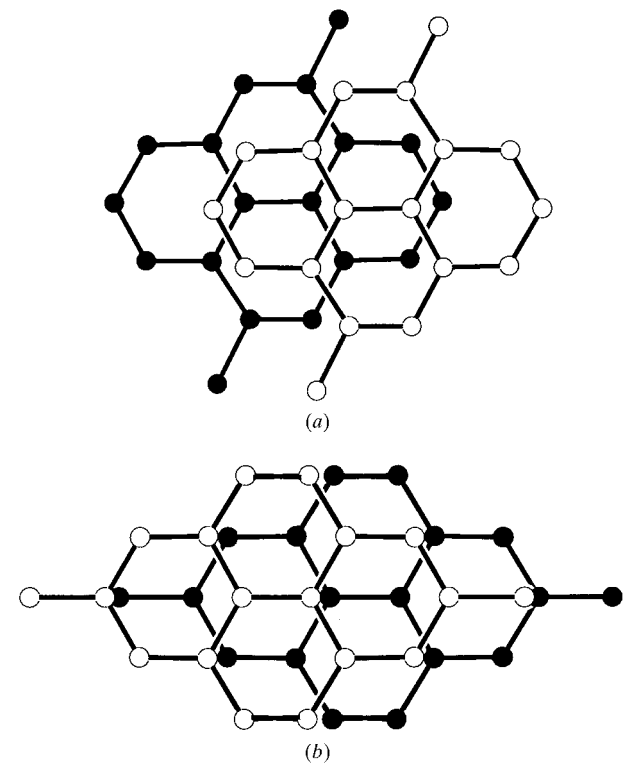

Fig. 9. Molecular overlap in crystals of (*a*) (1) and (*b*) (2).

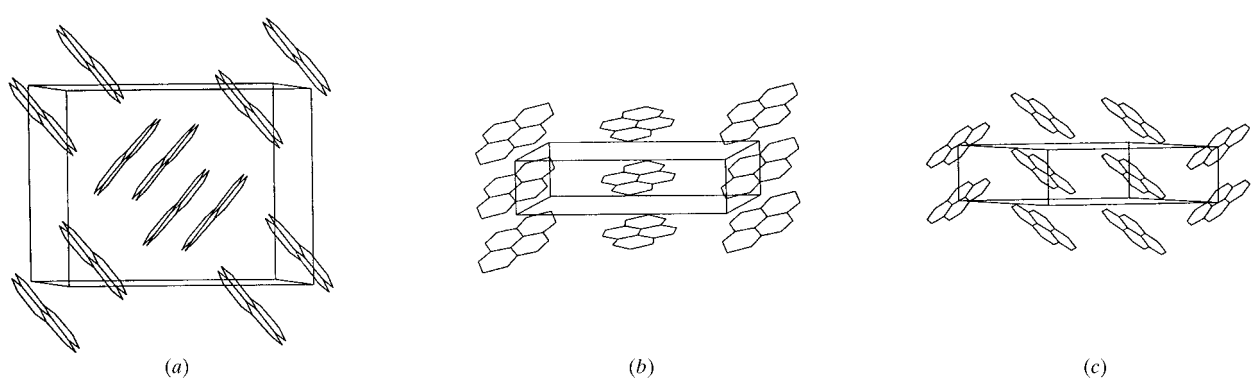

Fig. 8. Crystal-packing types: (*a*) sandwich-herringbone (SH) motif of decadeuteropyrene (Knight *et al.*, 1996); (*b*) β type, naphtho[1,8-*c*,*d*:4,5-*c′d′*]bis[1,2,6]selenadiazine (Gieren *et al.*, 1980); (*c*) γ type, 1,3,6,8-tetrafluoro-2,4,5,7,9,10-hexachloropyrene (Hazell & Weigelt, 1975) (F and Cl atoms omitted for clarity).

Table 6. *Parameters relevant for definition and classification of crystal-packing types for pyrenes and analogues*

Packing types are sandwich-herringbone (SH), β, γ and quasi-β types (β*, β**). p is the shortest crystallographic axis, d is the interplanar distance between parallel neighbouring rings and ν is the corresponding centre-to-centre offset (Å). φ is the angle between the p axis and the ring plane and θ is the interplanar angle betwen the adjacent stacks (°). S_1, S_2 and S_3 are stacking areas (Å^2). V is the interactive volume (Å^3). E is the average atomic electronegativity after Pauling. N is the number of delocalized, localized and free pair electrons. Q is the sum of the partial atomic charges of the pyrene skeleton (16 non-H atoms) calculated using *MOPAC-PM*3.

	Space group	Z	Packing type	p	φ	d	θ	ν	S_1	S_2	S_3	V	E	N	Q
PYRENE02	$P2_1/a$	4	SH	8.470 (10)	16.41 (3)	3.528 (3)	83.37 (4)	1.762	12.1	12.1	0	42.5	2.38	16	−1.047
pyrene†	$P2_1/a$	4	SH	8.22064 (1)	16.16 (15)	3.433 (6)	76.71 (7)	1.443	14.2	14.2	0	48.6	2.38	16	−1.047
VOXLOJ	$P2_1/n$	2	β	3.922 (1)	62.02 (13)	3.462 (12)	55.95 (19)	1.840	10.2	17.6	2.6	70.3	2.48	22	−0.956
DOXTEP	$P2_1/n$	2	β	4.026	60.06	3.489	59.88	2.009	10.4	19.6	1.8	72.8	2.41	22	−0.963
NAPTDZ10	$P2_1/a$	2	β	3.794 (4)	63.79 (7)	3.404 (2)	51.3 (1)	1.676	13.4	18.8	3.0	91.4	2.55	30	−0.525
NAPSEZ10	$P2_1/a$	2	β	3.863 (5)	62.32 (7)	3.420 (15)	49.32 (10)	1.782	13.8	19.5	3.7	91.8	2.54	30	−0.529
(1)	$P2_1/c$	2	β	4.0246 (5)	58.80 (5)	3.442 (18)	10.8 (2)	2.085	10.6	16.3	4.4	70.6	2.41	20	−0.864
(2)‡	$C2/m$	2	β	3.9615 (5)	64.34 (12)	3.571 (2)	0	1.715					2.41	20	−0.740
DMPYRN§	$P2_1/c$	4	SH	8.1554 (5)		3.45		1.909	8.8	8.8	0	30.5	2.37	16	−0.994
ELLAGC	$P2_1/c$	2	β	3.745	64.18 (5)	3.370 (6)	8.88 (7)	1.631	10.0	16.9	4.2	67.3	2.69	48	0.371
KENDEM	$P2_1/c$	2	γ	5.305 (1)	41.16 (3)	3.491 (2)	82.32 (5)	3.994	6.2	12.5	0	21.8	2.68	42	0.627
DAHNEF	$P2_1/c$	4	β	3.877 (1)	63.93 (5)	3.484 (6)	52.13 (7)	1.704	11.8	16.9	2.1	82.4	2.41	16	−0.960
TFHCPY10	$P2_1/a$	2	γ	4.864 (5)	45.18 (5)	3.450 (2)	89.64 (7)	3.429	4.4	8.5	0	15.3	2.89	76	−0.610
DECPYR10¶	$P2_1/n$	4	β*	7.494 (5)	82.46 (4)	3.715 (3)	15.08 (6)	2.8	5.4	7.0	3.8	19.9	2.77	76	−1.286
BUTPYR10††	$P\bar{1}$	1	—	6.138 (5)	32.42 (3)	3.292 (2)	0	5.181	0	0	0	0	2.34	16	−1.001
VAMZIS	$P2_1/a$	4	γ	5.018 (6)	43.03 (15)	3.424 (8)	86.1 (2)	3.668	1.7	3.4	0	5.9	2.42	16	−1.016
TAHBUZ‡‡	$P2_1/a$	4	β**	8.197 (2)	56.53 (6)	3.673 (8)	57.21 (9)	10.112					2.52	18	−0.956
ZEDDIV	Pa	2	γ	4.815 (1)	45.57 (3)	3.438 (6)	88.85 (8)	3.371	4.1	8.2	0	14.1	2.42	18	−0.968
KASZAF01	$P2_1/a$	2	β	3.795 (1)	63.33 (3)	3.390 (6)	34.52 (5)	1.269	15.3	20.3	10.4	103.9	2.44	20	−0.903

† Deuteropyrene (Knight *et al.*, 1996). ‡ Stacking areas are not calculated because of the disorder. § Missing coordinates (Ingartinger *et al.*, 1977, an entry from the CSD). ¶ Average values of ν and S_1. †† Non-aromatic packing type. ‡‡ Stacking areas are not calculated since the pyrene rings are not stacked with each other but with another aromatic system (salicylidene).

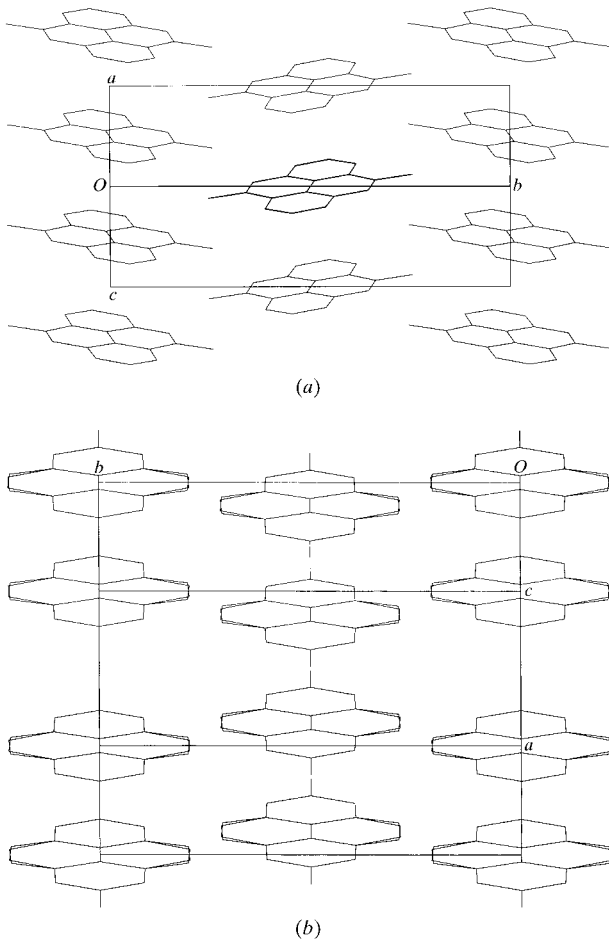

Fig. 10. Crystal packing of the β type in (*a*) (1) and (*b*) (2).

6, TFHCPY10). In the structure of (1), the presence of endocyclic nitrogen produces a small diagonal shift. The values of the offset parameter for (1) and (2) are 2.085 and 1.715 Å, respectively. The smaller value of this parameter in the structure of (2) can be explained by the disorder, which changes the orientation of the vector along the C4—N4 bond from one stacked molecule to the other. The short ν vector denotes dominating $\pi\cdots\pi$ interaction which characterizes β and SH types. The extremely short offset parameter of 1.269 Å in *N*,*N*′-disalicylidene-1,6-pyrenediamine (Table 6, KASZAF01, Fig. 2) is due to the stacks of pyrene and attached aromatic substituents. For the γ type a larger offset occurs ($3.37 < \nu < 3.99$ Å). The common characteristic for SH and γ types (Figs. 8*a* and 8*c*, Table 6) is an almost perpendicular orientation of the adjacent stacks ($\theta > 80^\circ$). The interactive volume and the overlapping surfaces (defined in Fig. 3) also illustrate the degree of $\pi\cdots\pi$ interaction. The interactive volume is largest for the β type ($67.3 < V < 103.9$ Å^3), smaller for SH ($30.5 < V < 48.6$ Å^3), and smallest for the γ type ($V < 21.8$ Å^3). The overlapping surfaces (Fig. 3) are very distinctive for a certain packing pattern. In the SH type with two molecules in a pair, $S_1 = S_2$ whereas $S_3 = 0$. In the β type with a high degree of $\pi\cdots\pi$ interaction, the overlapping surfaces between two molecules are large, particularly S_2, whereas the overlapping surfaces among the three closest neighbours S_3 are smaller than $S_1 + S_2$. For the γ type $S_2 > S_1$ and $S_3 = 0$ (Fig. 3, Fig. 8*c*). The geometrical parameters are sufficient to discriminate unambiguously among patterns as illustrated by Fig. 11.

However, from the correlations between the molecular characteristics, including the elements of electronic structure and crystal packing, additional information for

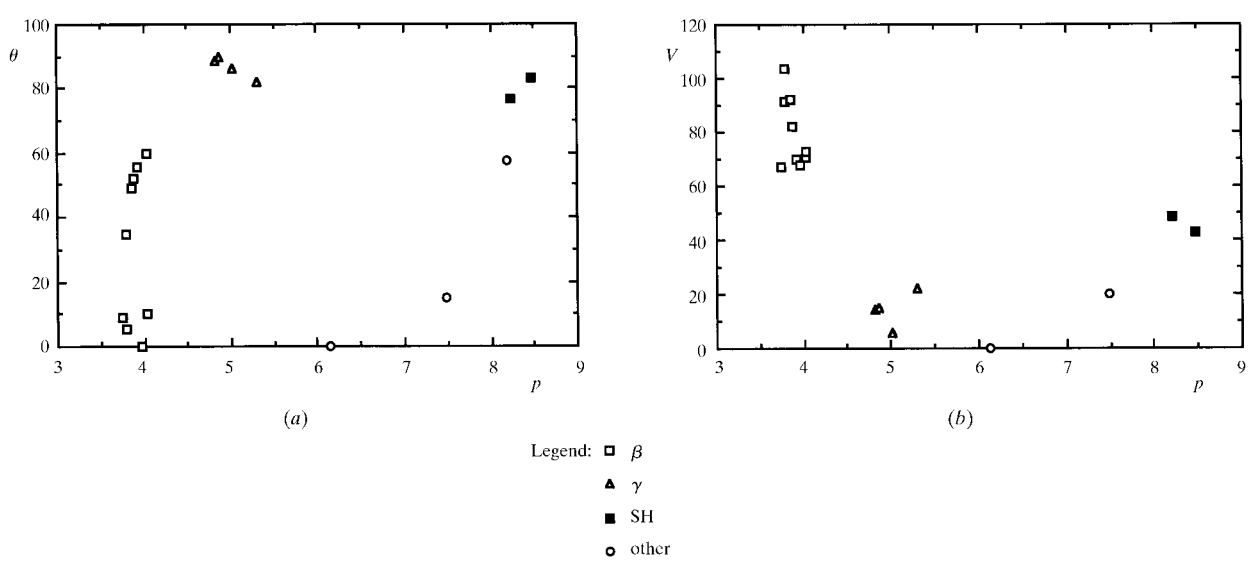

Fig. 11. Scatterplots used to discriminate specific packing types of pyrenes and analogues. (*a*) The shortest axis *versus* θ. (*b*) The shortest axis *versus* *V*.

classification of the packing patterns of these aromatics can be gained. Over forty relationships between the geometrical and the electronic structure parameters, based on second-order polynomial regression analysis, were examined and only those with correlation coefficients $r \geq 0.85$ were used: *V versus N* (Fig. 12*a*), *V versus E* (Fig. 12*b*) and S_2 *versus N* (Fig. 12*c*), S_2 *versus E* (Fig. 12*d*) reveal the optimal ranges of the electronic structure parameters for a certain packing pattern, being more restrictive for β than for γ types (Table 6). Moreover, a very narrow range of N and E can satisfy the SH packing arrangement.

Correlations of geometrical parameters S_1, S_2, V, ν and Q (Table 6, Figs. 13*a–d*) are shown. Comparison of both S_1 and S_2 *versus* Q shows a similar trend; the molecules to be stacked are limited by the values of their partial charges. In general, for β and even more for SH types with a high degree of π interactions, only narrow ranges of N, E and Q are tolerated. On the contrary, in the γ type there is no such close contact between neighbouring molecules which can be disturbed by repulsions and thus N, E and Q are distributed over a wide range.

Calculations of the potential energy between the relevant molecule and its neighbours at a maximum distance of 15 Å in the unit cell obtained using *PLUTO* (Motherwell, 1997) revealed that the lowest energies were obtained for stacked pairs in β and SH arrangements. However, this type of calculation should be treated with caution, since the parameterization should take care of intra- and intermolecular interactions, the contribution from which should be weighted individually for each type of molecule. For this reason, calculations were carried out only for crystals free from hydrogen bonds and polar groups. The calculations performed for diazapyrenes (1) and (2), both of β type, detected the lowest energy for the two closest molecules. Disorder in (2) changes the orientation of the C4*a*—N4 vector; instead of a small repulsion, attraction between stacked molecules occurs. For this reason, the offset parameter is smaller for (2) than for (1) (Table 6). The structure of (2) can be described by an infinite sequence of energetically well balanced *AB* layers. These results are in agreement with those obtained from *ab initio* calculations for a benzene dimer (Hobza *et al.*, 1994) which found the parallel-displaced structure to be

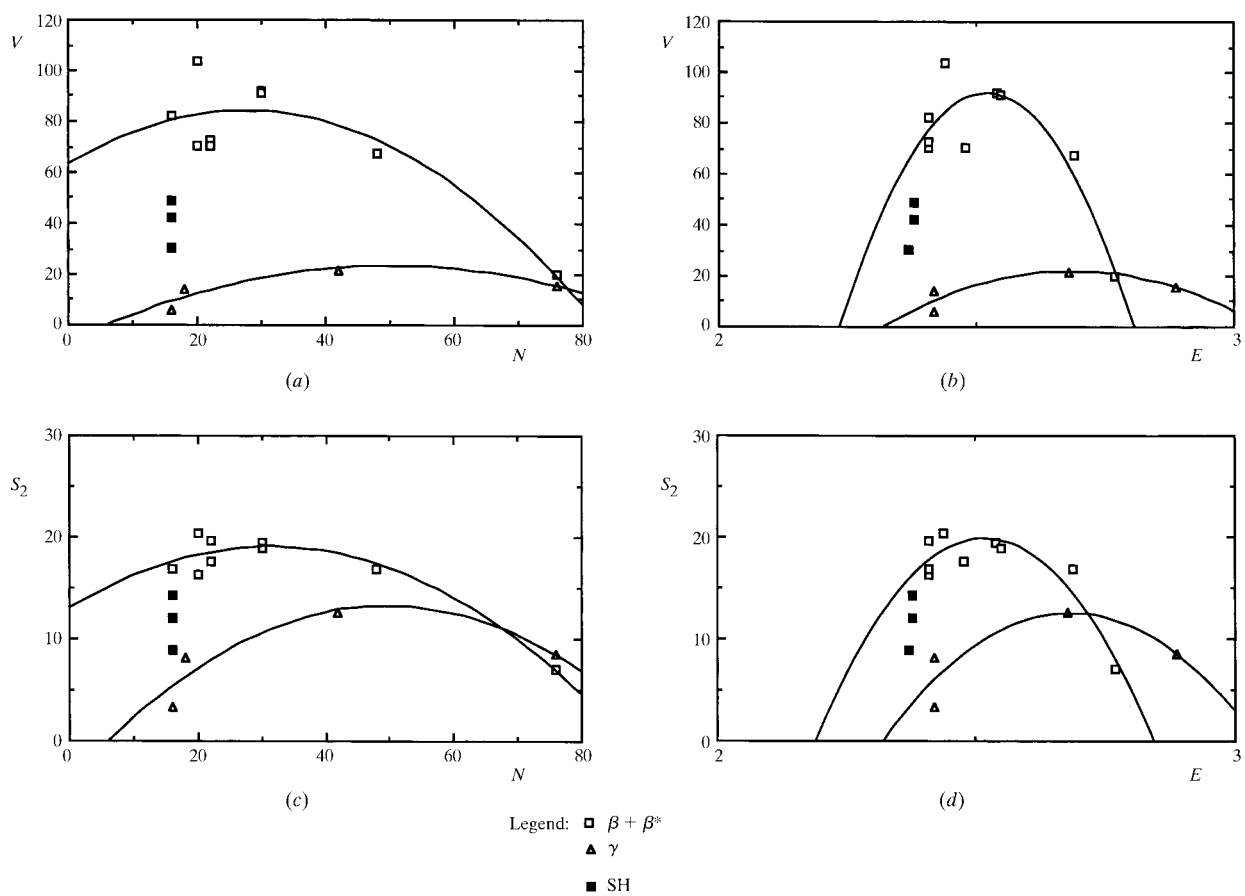

Fig. 12. Correlations of geometrical parameters V and S_2 (definitions given in Fig. 3) and electronic structures using parameters N and E (defined in Table 6) used to resolve the packing patterns. A second-order polynomial regression was used.

slightly more stable than the displaced T-shaped structures. The empirical rules of Hunter & Sanders (1990) are in favour of the T-shaped molecules. Recent calculations performed by Chipot *et al.* (1996) on benzene and toluene dimers in the gas phase and in an aqueous medium have not resolved the problem of orientational preference in general. However, these authors stress the importance of taking into account not only the electrostatic and dispersion interactions between the aromatic moieties but possible steric hindrance, particularly in analysing $\pi\cdots\pi$ interactions in proteins. Steric hindrance caused by the bulky *tert*-butyl groups disables stacking in the crystal structure of 2,7-di-*tert*-butylpyrene (BUTPYR10, Fig. 2, Table 6). This evidence also supports the observations of Chipot *et al.* (1996).

In order to learn more about the $\pi\cdots\pi$ interactions of pyrene and analogues, a search for molecular complexes with other aromatic molecules was performed using the CSD. Of about 40 complexes detected, only those of the highest accuracy ($R \leq 0.07$) were selected according to the criteria described in §2.4. The examination of their structures reveals stacking of pyrene and aromatic molecules in an *AB* sequence with $d \simeq 3.50$ Å (where d is the distance between the centres of mass). Formation of such molecular complexes can be considered as interaction between π-donor HOMOs and π-acceptor LUMOs of molecules in alternating layers in the unit cell (Bleidelis *et al.*, 1976; Purcell & Kotz, 1977), which can be treated as charge-transfer complexes (Zacharias *et al.*, 1991). Some of these molecular adducts are of interest as DNA intercalators. The charged diazaprenium species can be as good intercalators as ethidium (Steiner-Biočić *et al.*, 1996; Sarfati *et al.*, 1995; Meyer-Almes & Porschke, 1993). On the other hand, stable adducts with layered structures can be anisotropic conductors of electricity; current flows easily normal to the molecular planes but negligibly in directions parallel to the aromatic planes (one-dimensional organic 'metals').

4. Conclusions

Classification of the crystal packing of aromatic hydrocarbons derived by Gavezzotti & Desiraju (1988) and Desiraju & Gavezzotti (1989) using geometrical parameters is applicable to the pyrenes, diazapyrenes and

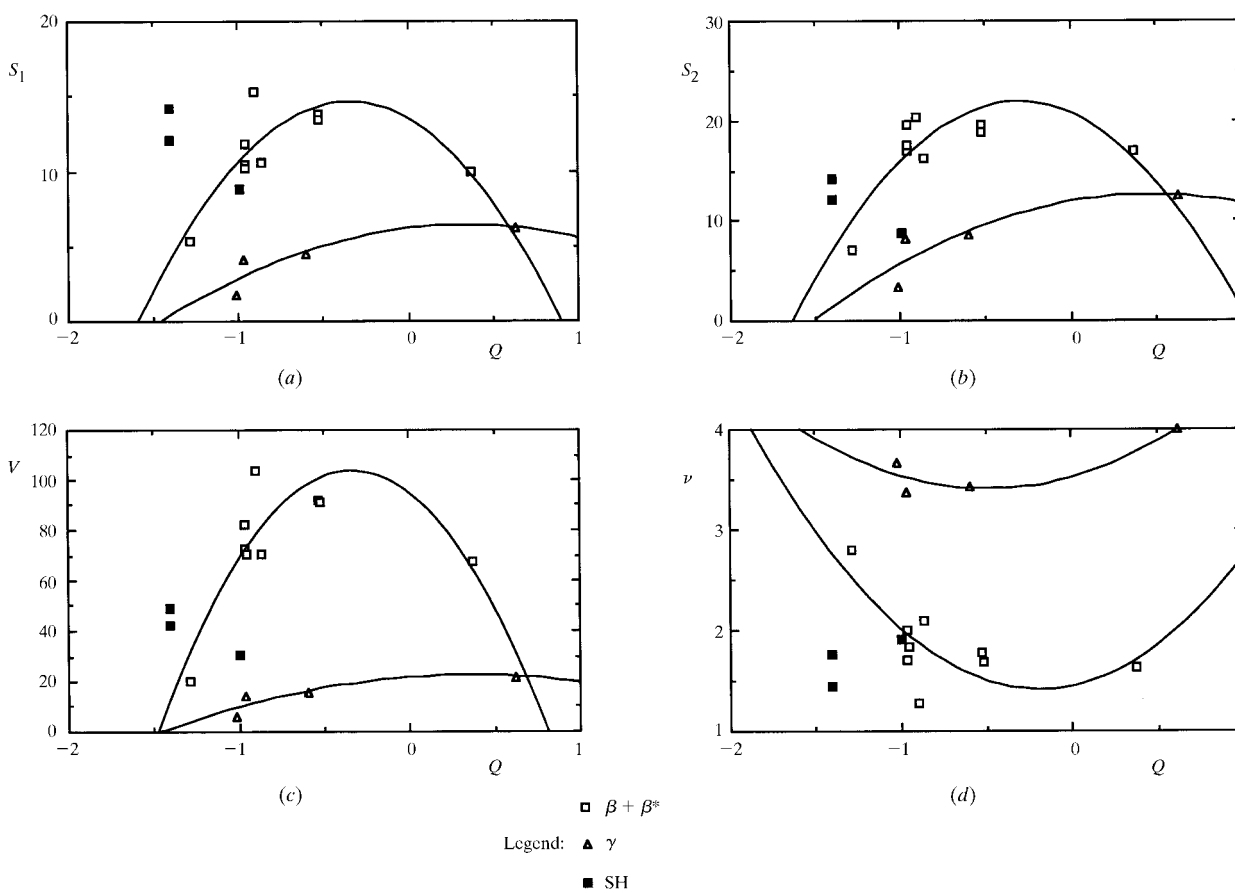

Fig. 13. Correlations of geometrical parameters (defined in Fig. 3) S_1, S_2, V, ν and Q (definitions in Table 6). A second-order polynomial regression was used.

analogous conjugated systems. Correlations of geometrical and electronic structure parameters relate properties of molecular and crystal structures:

(i) plots of interactive volume V *versus* average electronegativity E, and overlapping surface S_2 *versus* E, reveal that for maximum values of V and S_2 the average electronegativity is about 2.5 and characterizes the β packing type (E for graphite is 2.5);

(ii) plots of overlapping surfaces and interactive volume *versus* the sum of partial atomic charges, Q, show that $Q \simeq 0$ when V and S_2 are at a maximum (for graphite, $Q = 0$).

From these correlations, a comparison between graphite and β-type packing is possible. Thus, the β type can be described as the packing motif with a high degree of $\pi\cdots\pi$ interactions. Most of the compounds analysed reveal crystal packing of the β type characterized by stacked displaced layers with a high contribution of $\pi\cdots\pi$ interactions. The high predominance of the single space group ($P2_1/c$) detected in the crystal packing with defined parameters of the classification of the packing patterns make these molecules good candidates for crystal structure prediction. However, the main obstacle still remains of the feasible energetic evaluation of the proposed model (van Eijck & Kroon, 1997).

This work was carried out with the financial support of the Ministry of Science, Republic of Croatia.

References

Allen, F. H. & Kennard, O. (1993). *Chem. Des. Autom. News*, **8**, 31–37.

Allinger, N. L. (1992). *MM*3(92). Technical Utilization Corporation, Powell, Ohio, USA.

Allinger, N. L., Tai, J. C. & Stuart, T. W. (1967). *Theor. Chim. Acta*, **8**, 101–116.

André, I., Foces-Foces, C., Cano, F. H. & Martinez-Ripoll, M. (1997*a*). *Acta Cryst.* B**53**, 984–995.

André, I., Foces-Foces, C., Cano, F. H. & Martinez-Ripoll, M. (1997*b*). *Acta Cryst.* B**53**, 996–1005.

Badger, G. M. & Sasse, W. F. H. (1957). *J. Chem. Soc.* pp. 4–8.

Bailly, C., OhUgin, C., Rivalle, C., Bisagui, E., Henichart, J.-P. & Waring, M. (1990). *J. Nucleic Acid Res.* **18**, 6283–6291.

Blacker, A. J., Jazwinski, J. & Lehn, J.-M. (1987). *Helv. Chim. Acta*, **70**, 1–12.

Blacker, A. J., Jazwinski, J., Lehn, J.-M. & Wielhelm, F. X. (1986). *J. Chem. Soc. Chem. Commun.* pp. 1035–1037.

Bleidelis, Ya., Shvets, A. E. & Freimans, Ya. F. (1976). *Zh. Strukt. Khim.* **17**, 1096–1110.

Brunn, A. M. & Harriman, A. (1991). *J. Am. Chem. Soc.* **113**, 8153–8159.

Chipot, C., Jaffe, R., Maigret, B., Pearlman, D. A. & Kollman, P. (1996). *J. Am. Chem. Soc.* **118**, 11217–11224.

Denny, W. A., Baguley, B. C., Cain, B. F. & Waring, M. J. (1983). In *Molecular Aspects of Anticancer Drug Action*, edited by S. Niedle and M. J. Waring, Vol. 2, pp. 1–34. Weinheim: VCH.

Desiraju, G. R. & Gavezzotti, A. (1989). *J. Chem. Soc. Chem. Commun.* pp. 621–623.

Dewar, M. J. S., Healy, E. F. & Yuan, Y.-C. (1990). *J. Comput. Chem.* **11**, 541–542.

Dewar, M. J. S. & Thiel, W. (1977). *J. Am. Chem. Soc.* **99**, 4899–4907.

Dewar, M. J. S., Zoebisch, E. G., Healy, G. F. & Stewart, J. J. P. (1985). *J. Am. Chem. Soc.* **107**, 3902–3909.

D'Souza, L. J. & Maitra, U. (1996). *J. Org. Chem.* **61**, 9494–9502.

Eijck, B. P. van & Kroon, J. (1997). *J. Comput. Chem.* **18**, 1036–1042.

Enraf–Nonius (1992). *CAD*-4 *EXPRESS*. Enraf–Nonius, Delft, The Netherlands

Fairfull, A. E. S., Peak, D. A., Short, W. F. & Watkins, T. I. (1952). *J. Chem. Soc.* pp. 4700–4709.

Gavezzotti, A. (1994). *Acc. Chem. Res.* **27**, 309–314.

Gavezzotti, A. & Desiraju, G. R. (1988). *Acta Cryst.* B**44**, 427–434.

Gieren, A., Lamm, V., Haddon, R. C. & Kaplan, M. L. (1980). *J. Am. Chem. Soc.* **102**, 5070–5073.

Goddard, R., Haenel, M. N., Herndon, W. C., Krüger, C. & Zander, M. (1995). *J. Am. Chem. Soc.* **117**, 30–41.

Hazell, A. C. & Jagner, S. (1976). *Acta Cryst.* B**32**, 682–686.

Hazell, A. C., Larsen, F. K. & Lehmann, M. S. (1972). *Acta Cryst.* B**28**, 2977–2984.

Hazell, A. C. & Weigelt, Å. (1975). *Acta Cryst.* B**31**, 2891–2893.

Herndon, W. C. (1974). *J. Am. Chem. Soc.* **96**, 7605–7614.

Herndon, W. C. & Párkányi, C. (1976). *J. Chem. Educ.* **53**, 689–692.

Hobza, P., Selzle, H. L. & Schlag, E. W. (1994). *J. Am. Chem. Soc.* **116**, 3500–3506.

Hunter, C. A. (1994). *Chem. Soc. Rev.* pp. 101–109.

Hunter, C. A. & Sanders, K. M. (1990). *J. Am. Chem. Soc.* **112**, 5525–5534.

Ingartinger, N., Kirrstetter, R. G. H., Krieger, C., Rodewald, N. & Staab, H. A. (1977). *Tetrahedron Lett.* pp. 1425–1428.

Johnson, C. K. (1976). *ORTEP*II. Report ORNL-5138. Oak Ridge National Laboratory, Tennessee, USA.

Kiralj, R., Kojić-Prodić, B., Nikolić, S. & Trinajstić, N. (1998). *J. Mol. Struct. (Theochem.)*, **427**, 25–37.

Kiralj, R., Kojić-Prodić, B., Žinić, M., Alihodžić, S. & Trinajstić, N. (1996). *Acta Cryst.* B**52**, 823–837.

Kitaigorodsky, A. I. (1973). *Molecular Crystals and Molecules.* New York: Academic Press.

Knight, K. S., Shanklund, K., David, W. I. F., Shanklund, N. & Love, S. W. (1996). *Chem. Phys. Lett.* **258**, 490–494.

Meyer-Almes, F. J. & Porschke, D. (1993). *Biochemistry*, **32**, 4246–4253.

MOPAC (1990). *MOPAC*. Version 6.00. Frank Seiler Research Laboratory, Air Force Academy, Colorado Springs, Colorado 80840, USA.

Mosby, W. L. (1957). *J. Org. Chem.* **22**, 671–673.

Motherwell, W. D. S. (1997). *PLUTO*. Implemented in the Cambridge Structural Database, version 5.13. Cambridge Crystallographic Data Centre, 12 Union Road, Cambridge, England.

Pauling, L. (1980). *Acta Cryst.* B**36**, 1898–1901.

Piantanida, I. (1997). MSc thesis, Faculty of Science, University of Zagreb, Croatia.

Purcell, K. F. & Kotz, J. C. (1977). *Inorganic Chemistry*, pp. 159, 197. Philadelphia: Saunders Co.

Robertson, J. M. (1951). *Proc. R. Soc. Chem. London Ser. A*, **207**, 101–110.
Sarfati, R. S., Berthod, T., Guerreiro, C. & Canard, B. (1995). *J. Chem. Soc. Perkin Trans.* 1, pp. 1163–1171.
Sheldrick, G. M. (1990). *Acta Cryst.* A**46**, 467–473.
Sheldrick, G. M. (1993). *SHELXL*93. *Program for the Refinement of Crystal Structures.* University of Göttingen, Germany.
Shriver, D. F., Atkins, T. W. & Langfors, C. H. (1990). *Inorganic Chemistry*, pp. 640–641. New York: Freeman.
Sobell, H. M., Tsai, C.-C., Jain, S. C. & Gilbert, S. G. (1977). *J. Mol. Biol.* **114**, 333–365.
Spek, A. L. (1990*a*). *Acta Cryst.* A**46**, C-34.
Spek, A. L. (1990*b*). *HELENA. Program for Data Reduction.* University of Utrecht, The Netherlands.
Spek, A. L. (1991). *PLUTON. Molecular Graphics Program.* University of Utrecht, The Netherlands.
Sponer, J. & Hobza, P. (1996). *Int. J. Quantum Chem.* **57**, 959–970.
Sponer, J., Lesczynski, J. & Hobza, P. (1996). *J. Phys. Chem.* **100**, 5590–5596.
Stat Works (1988). *CricketGraph Software.* Version 1.3. Stat Works, Malvern, Pennsylvania, USA.
Steiner-Biočić, I., Glavaš-Obrovac, Lj., Karner, I., Piantanida, I., Žinić, M., Pavelić, K. & Pavelić, J. (1996). *Anticancer Res.* **16**, 3705–3708.
Stewart, J. J. P. (1989*a*). *J. Comput. Chem.* **10**, 209–220.
Stewart, J. J. P. (1989*b*). *J. Comput. Chem.* **10**, 221–264.
Stewart, J. J. P. (1990*a*). *J. Comput. Chem.* **11**, 543–544.
Stewart, J. J. P. (1990*b*). *J. Comput.-Aided Mol. Des.* **4**, 1–105.
Veal, J. M., Li, Y., Zimmerman, S. C., Lamberson, C. R., Cory, M., Zon, G. & Wilson, W. D. (1990). *Biochemistry*, **29**, 10918–10927.
Wakelin, L. P. G. (1986). *Med. Res. Rev.* **6**, 275–340.
Webb, T. H. & Wilcox, C. S. (1993). *Chem. Soc. Rev.* pp. 383–395.
Wells, A. F. (1975). *Structural Inorganic Chemistry*, 4th ed., p. 734. Oxford: Clarendon Press.
Wilson, W. D. (1989). In *Nucleic Acids in Chemistry and Biology*, edited by M. Blackburn and M. Gait. Oxford: IRL Press.
Wilson, W. D., Strebowski, L., Tanious, F. A., Watson, R. A., Mokrosz, J. L., Strekowska, A., Webster, G. D. & Niedle, S. (1988). *J. Am. Chem. Soc.* **110**, 8292–8299.
Zacharias, D. E., Prout, K., Myers, C. B. & Glusker, J. P. (1991). *Acta Cryst.* B**47**, 97–107.